
Contact Stress Analysis of a Spur Gear Using Lewis and Hertz Theory

Than Zaw Oo¹, Htay Htay Win², War War Min Swe³, Yin Yin Aye⁴

thanzawoo2341993@gmail.com, htayhtayw@gmail.com, warswe05@gmail.com, dryinn2025@gmail.com

^{1,2,3,4} Department of Mechanical Engineering, Mandalay Technological University, Myanmar.

Article Information

Received : 9 Apr 2026

Revised : 16 Apr 2026

Accepted : 23 Apr 2026

Keywords

Spur Gear Set,
AGMA Contact
Stress, Changing
Face Widths,
FEA

Abstract

This paper focuses on the design and contact stress analysis of a spur gear for sugarcane juice extraction machine by changing gear face widths and three different materials (ASTM A 220-99, ASTM A 536-84 and C54400). Gear corrosion occurs at contact points as a result of bending stress and contact stress. This is the major source of the gear failure of the sugarcane juice extraction machine. This whole mechanism will be driven by a 1383W capacitor-start induction motor according to the motor power selection. Pitch diameters of 48 mm and module of 2.5 mm spur gear is selected in the design of gear. In theoretical analysis, the Lewis contact stress equation is used. In the numerical analysis, the geometry is created by SolidWorks software. The minimum von-Mises stress and effective strain are found that on ASTM A 220-99 material by using ANSYS 2020 R1 software. In this paper, von-Mises stress and effective strain are analyzed by changing the face widths of gears to 13 mm, 15 mm, 17 mm, 19 mm and 21 mm and using finite element analysis (FEA). Although all face widths are safe for this design, 17 mm is chosen in this paper due to power consumption and strength points of view.

A. Introduction

Sugarcane is a tropical grass that is the primary source of sugar production worldwide. It's grown in tropical and subtropical regions due to its need for a warm climate and plenty of water. The plant is known for its tall, jointed stalks which contain a large amount of sucrose, making it ideal for extracting sugar and other by-products like molasses and ethanol[1].

A sugarcane juice extraction machine is designed to efficiently extract juice from sugarcane stalks. These machines come in various types and sizes, typically consisting of rollers or crushers that press the cane to extract the juice. They are commonly used in small-scale operations, such as juice stalls, as well as in larger commercial settings[2].

Sugarcane juice is a refreshing, naturally sweet beverage made from pressing fresh sugarcane stalks. It's popular in many tropical and subtropical regions due to its delicious taste and health benefits. The main components of a sugarcane extraction machine include rollers, spur gears, motor, metal frame and bearing[6].

Sugarcane is a species of tall, perennial grass that is used for sugar production. Sugarcane contains important vitamins and minerals (iron, magnesium, vitamin B1 and riboflavin). Sugarcane juice extraction machine has prominent features such as beautiful shape, easy operation, low investment, and high production juice[7].

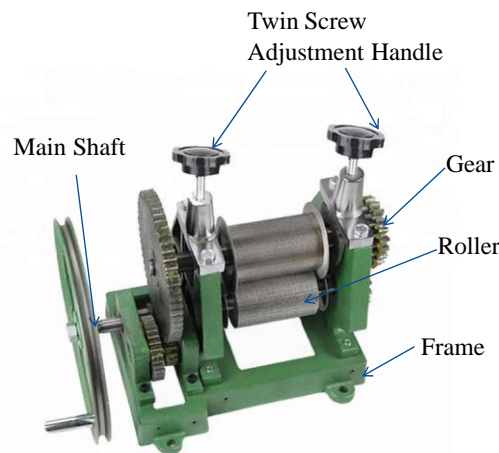


Figure 1. Sugarcane Juice Extraction Machine

This machine employs spur pinions and gears to achieve a specific speed and output capacity. There is transmission gear, spur gears and shaft.

The gears are generally used to transmit power and torque [8]. Surface wear, tooth bending fatigue, contact fatigue, and scoring are the four main ways that gear systems fail [9]. When the two gears come into touch at the contact point, a very high stress is created that the material is unable to handle. The torque and power of a spur gear are computed using the tangential force component. The gear receives contact stress and bending stress because of the tangential load acting on the gear. Gear failure occurs when contact stress on the gear exceeds the wear strengths of the gear material; this is known as wear or cracking failure of the gear. The contact

stresses were computed using the Hertzian equation and finite element analysis [10].

B. Research Method

There are three steps to solve the spur gear set failure in the sugarcane juice extraction machine. The first step is to design the spur gear and calculate the equivalent stress and strain of the spur gear set by using Hertz theory and the Lewis formula. The second step is to analyze the structural behaviors of the spur gear set with ANSYS 2020 R1 software by changing materials and face widths. The third step is to choose the suitable material and face width for the spur gear set.

C. Design Consideration of Spur Gears

The pitch circle of a spur gear is the circle that represents the size of the corresponding friction roller that could replace the gear. When two gears mesh, they have tangent pitch circles, and their points of contact are on the line that joins their centers. The gear’s pitch diameter, D_p , is simply the diameter of the pitch circle shown in Figure 2. However, because the pitch circle is located near the middle of the gear teeth, the pitch diameter cannot be measured directly from the gear. The number of teeth, T_g , is simply the total number of teeth on the gear [11].

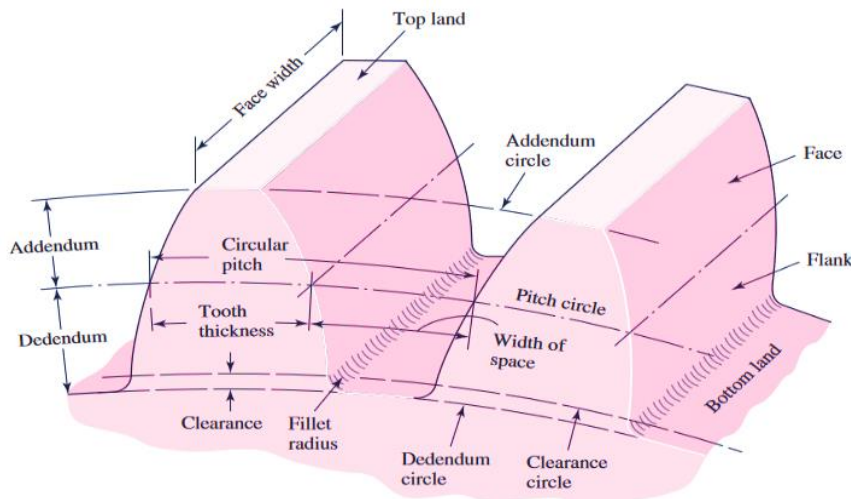


Figure 2. Teeth of Spur Gear [12]

Table 1. Specifications of Gears

Types of gear	Number of Teeth, T_g	Module, m (mm)
Pinoin Gear 1	16	2.5
Gear 1	32	2.5
Pinoin Gear 2	16	3
Gear 2	64	3
Gear 3	18	4
Gear 4	18	4
Gear 5	21	4
Gear 6	21	4

The whole mechanism was driven by a 1383W capacitor-start induction motor. The motor speed (N) was 1450rpm, motor pulley diameter was 270 mm and machine pulley diameter was 75mm. The speed of pulley and gears were calculated

according to this velocity ratio Equation (1),

$$VR = \frac{T_2}{T_1} = \frac{D_2}{D_1} = \frac{N_1}{N_2} \tag{1}$$

Firstly, the pressure angle of the roller gear set (ϕ) is 14.5 and the velocity ratio is the ratio between the velocity of driver and driven gear. They can be calculated by using Equation (1). The pitch diameter of all gears can be calculated by using Equation (2) [13].

Pitch diameter, $D_p = T_g m$ (2)

The tip diameter and root diameters of the gears are shown in Equations (3) and (4) [14].

Tip diameter, $D_t = D_p + 2m$ (3)

Root diameter, $D_r = D_p - 2.5m$ (4)

The circular pitch (p) can be calculated from the number of teeth (N_t) and the pitch diameter of a gear (D_p).

$$p = \pi m = \frac{\pi N_t}{D_p} \tag{5}$$

The tooth thickness (t) is, $t = \frac{p}{2}$ (6)

Table 2. Result of Spur Pinions and Gears

Types of gear	Speed, N (rpm)	Pitch diameter D_p (mm)	Tip diameter D_t (mm)	Root diameter D_r (mm)	Circular pitch p (mm)	Tooth thickness t (mm)
Pinoin Gear 1	403	40	45	33.75	7.85	3.93
Gear 1	201.5	80	85	73.75	7.85	3.93
Pinoin Gear 2	201.5	48	54	40.5	9.42	4.71
Gear 2	50.375	192	198	184.5	9.42	4.71
Gear 3	50.375	72	80	62	12.57	6.29
Gear 4	50.375	72	80	62	12.57	6.29
Gear 5	50.375	84	92	74	12.57	6.29
Gear 6	50.375	84	92	74	12.57	6.29

Torque transmitted by gear (T) is 22.95Nm and the actual tangential tooth load for spur gear (W_t) is 765.49N by using Equation (7) [15],

$$W_t = \frac{2T}{D_p} \tag{7}$$

Contact Stress Calculation Using AGMA Equation

ASTM A 220-99, ASTM A 536-84, and C54400 are used for this research. These three materials have good wear resistance properties, excellent machinability, and tooth hardness. The mechanical properties of these materials are shown in Table 3.

Table 3. Material Properties of Spur Gear [16]

Materials	Density (ρ), kg/m ³	Yield Strength (S_y), MPa	Tensile Strength (S_{ut}), MPa	Young's Modulus, GPa	Poisson's ratio
Cast Iron (ASTM A 220-99)	7480	276	414	179	0.26
Cast Iron (ASTM A 536-84)	7480	276	414	179	0.26
Bronze (C54400)	7870	393	496	103	0.34

Table 4. Values of Parameters Used in AGMA Equations [17]

Parameter	Symbol	Value
Over load factor	k_o	1
Dynamic factor	k_v	1
Size factor	k_s	1
Load correction factor	C_{mc}	1
Pinion proportion modifier	C_{pm}	1
Mesh alignment correction factor	C_e	1
Over load factor	k_o	1
Dynamic factor	k_v	1
Size factor	k_s	1
Load correction factor	C_{mc}	1
Pinion proportion modifier	C_{pm}	1

Pinion proportion factor, $C_{pf} = \frac{b}{10D_p} - 0.025 = -0.001$ (8)

Mesh alignment factor, $C_{ma} = A + Bb + Cb^2 = 0.3292$ (9)

Load-distribution factor, $k_h = 1 + C_{mc}(C_{pf}C_{pm} + C_{ma}C_e) = 1.3282$ (10)

The geometry factor Z_I can be calculated as in Equation (11),

$$Z_I = \frac{\cos\phi \sin\phi}{2} \frac{VR}{VR + 1} = 0.13$$
 (11)

Z_E is the elasticity coefficient can be written as in Equation (12) [18],

$$Z_E = \left[\frac{1}{\pi \left(\frac{1 - \gamma_p^2}{E_p} + \frac{1 - \gamma_g^2}{E_g} \right)} \right]^{\frac{1}{2}} = 5.266\sqrt{\text{MPa}}$$
 (12)

Where γ and E are the Poisson's ratio and modulus of elasticity, respectively. The following Equation (13) is the contact stress equation by AGMA standard which is based on the Hertzian theory [19]:

$$\sigma_c = Z_E \sqrt{W_t \times k_o \times k_v \times k_s \times \frac{k_h}{D_p b} \times \frac{Z_R}{Z_I}} = 7.114\text{MPa}$$
 (13)

Where k_o , k_v , k_s , and k_h are the overload factor, dynamic factor, size factor, and load distribution factor, respectively. Firstly, face width (b) is 17 mm used and, Z_R , and Z_I are surface condition factor, and geometry factor for pitting resistance.

Calculation of Effective Stress and Strain

According to the Lewis formula, gear teeth are considered a cantilever beam with a tangential tooth load, W_t , applied at the tip. The radial component is negligible. The load is distributed uniformly across the full-face width. Forces due to the tooth sliding friction are negligible. The stress concentration in the tooth fillet is negligible [20]. The starting torque of the motor is 22.95Nm and the shear stress (τ_{xy}) can be calculated by using equation (14).

$$\tau_{xy} = \frac{16T}{\pi D^3} = 0.0509 \text{MPa} \quad (14)$$

Principal stresses are,

$$\sigma_{1,2} = \frac{1}{2}(\sigma_x + \sigma_y) \pm \frac{1}{2}\sqrt{(\sigma_x - \sigma_y)^2 + 4\tau_{xy}^2} \quad (15)$$

$$\sigma_1 = 7.127 \text{MPa}, \sigma_2 = -0.0134 \text{MPa}$$

von-Mises Stress or Effective Stress is,

$$\bar{\sigma} = \frac{1}{\sqrt{2}}[(\sigma_1 - \sigma_2)^2 + (\sigma_2 - \sigma_3)^2 + (\sigma_3 - \sigma_1)^2]^{\frac{1}{2}} = 7.134 \text{MPa} \quad (16)$$

First principal strain is, $\varepsilon_1 = \frac{1}{E}[\sigma_1 - \nu(\sigma_2 + \sigma_3)] = 4.321 \times 10^{-5} \quad (17)$

Second principal strain is, $\varepsilon_2 = \frac{1}{E}[\sigma_2 - \nu(\sigma_1 + \sigma_3)] = -1.002 \times 10^{-5} \quad (18)$

Third principal strain is, $\varepsilon_3 = \frac{1}{E}[\sigma_3 - \nu(\sigma_1 + \sigma_2)] = -9.916 \times 10^{-6} \quad (19)$

Effective strain is, $\bar{\varepsilon} = \left[\frac{2}{3}(\varepsilon_1^2 + \varepsilon_2^2 + \varepsilon_3^2)\right]^{\frac{1}{2}} = 3.711 \times 10^{-5} \quad (20)$

Calculation Contact Stress and Strain Using FEA

Stress state analysis of an elastic body with a complex shape, like a gear, is frequently performed using the finite element approach [21]. In the numerical analysis, structural behaviors (von-Mises stress and effective strain) of gear set are analyzed by changing (13,15,17,19,21) mm face widths spur gears by using ANSYS software. The solid model of (13,15,17,19,21) mm face widths spur gears set is created by SolidWorks software. The 3D model of spur gear set is as shown in Figure 4. This geometry model is meshed with high smoothing shown in Figure 5. The generated mesh is done by fine position to obtain the good quality of mesh and the number of nodes and elements are 22926 and 4110, respectively.

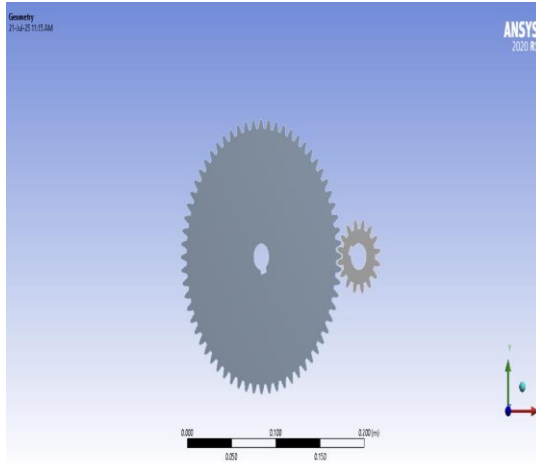


Figure 4. Geometry of Spur Gear Set

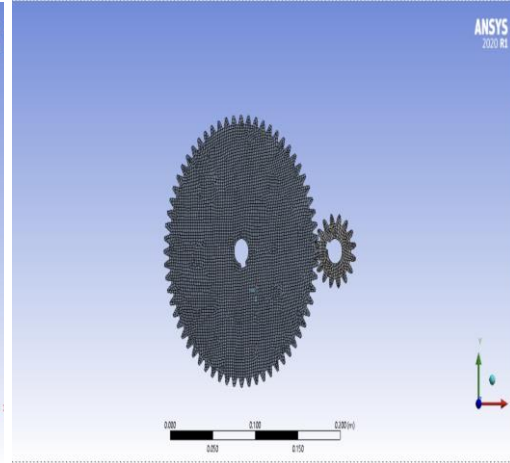


Figure 5. Meshing of Spur Gear Set

The boundary condition of the spur gear set is shown in Figure 6. The fixed point is set at the hub of the driving spur gear, while frictionless support is applied to the surface of the driven spur gear. The actual transmitted tooth load (F_t) of 765.492 N is applied in the X-direction on the surface of the driving spur gear tooth, with a turning moment of 22.95 Nm.

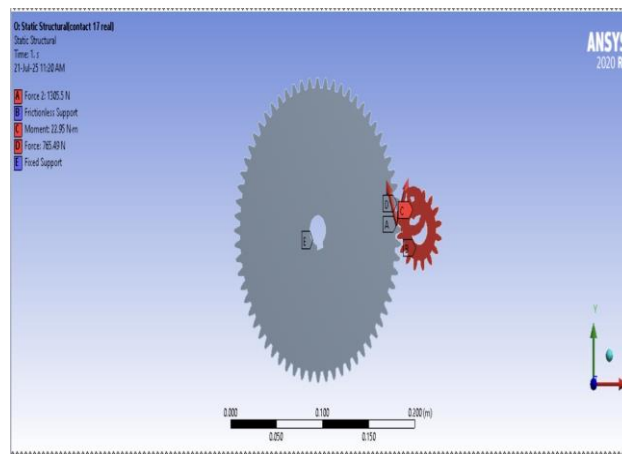


Figure 6. Boundary Condition of For Spur Gear Set

After finishing, set up the boundary conditions on the spur gear set, run the solution, and get the results for the structural behaviors of face widths gear set. In the numerical analysis of (13,15,17,19,21) mm face widths gear set using (ASTM A 220-99) cast iron.

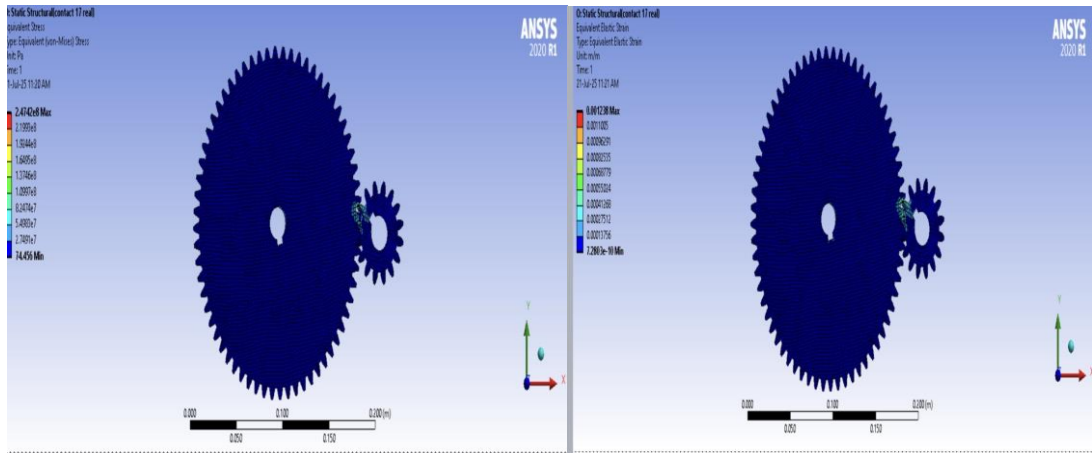


Figure 7. Equivalent Contact Stress and Strain (ASTM A 220-99)

In the numerical analysis of a 13 mm face width spur gear set using (ASTM A 220-99) cast iron, the maximum von-Mises stress of the spur gear set is 297.65 MPa and the maximum effective strain is 1.492×10^{-3} .

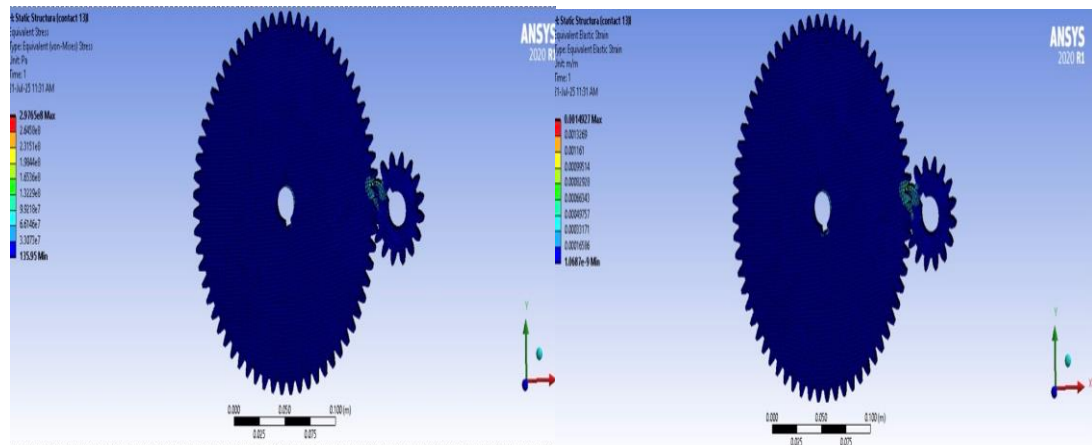


Figure 8. Equivalent Contact Stress and Strain (ASTM A 220-99)13 mm face width

In the numerical analysis of 15 mm face width spur gear set using (ASTM A 220-99) cast iron, the maximum von-Mises stress of spur gear set is 268.14 MPa and maximum effective strain is 1.343×10^{-3} .

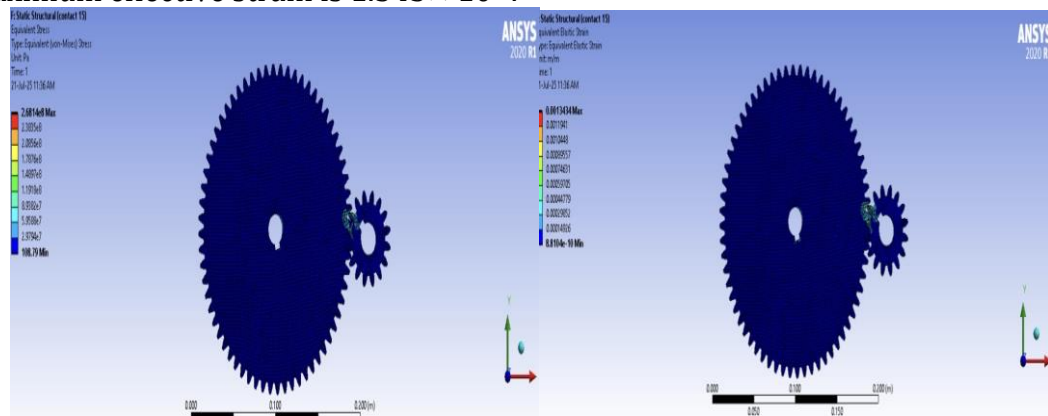


Figure 9. Equivalent Contact Stress and Strain (ASTM A 220-99)15 mm face width

In the numerical analysis of 17 mm face width spur gear set using (ASTM A 220-99) cast iron, the maximum von-Mises stress of spur gear set is 247.42 MPa and maximum effective strain is 1.238×10^{-3} .

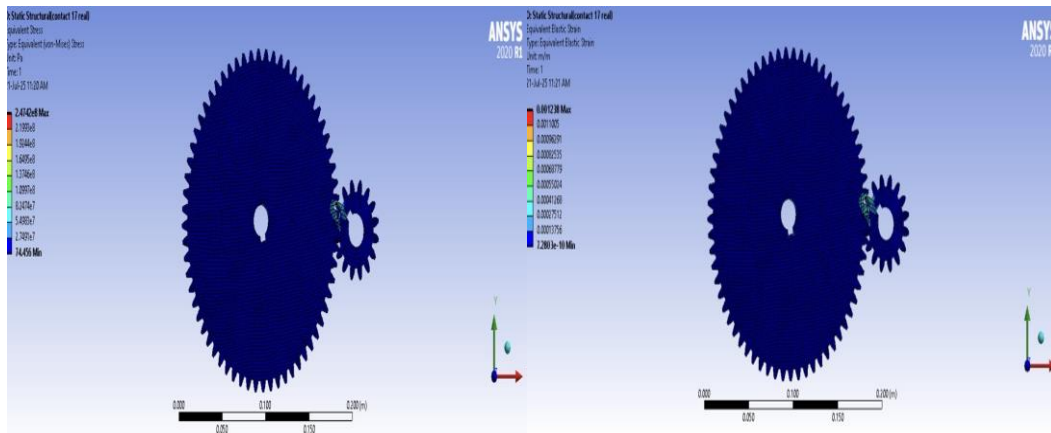


Figure 10. Equivalent Contact Stress and Strain (ASTM A 220-99)17 mm face width

In the numerical analysis of 19 mm face width spur gear set using (ASTM A 220-99) cast iron, the maximum von-Mises stress of spur gear set is 240.67 MPa and maximum effective strain is 1.214×10^{-3} .

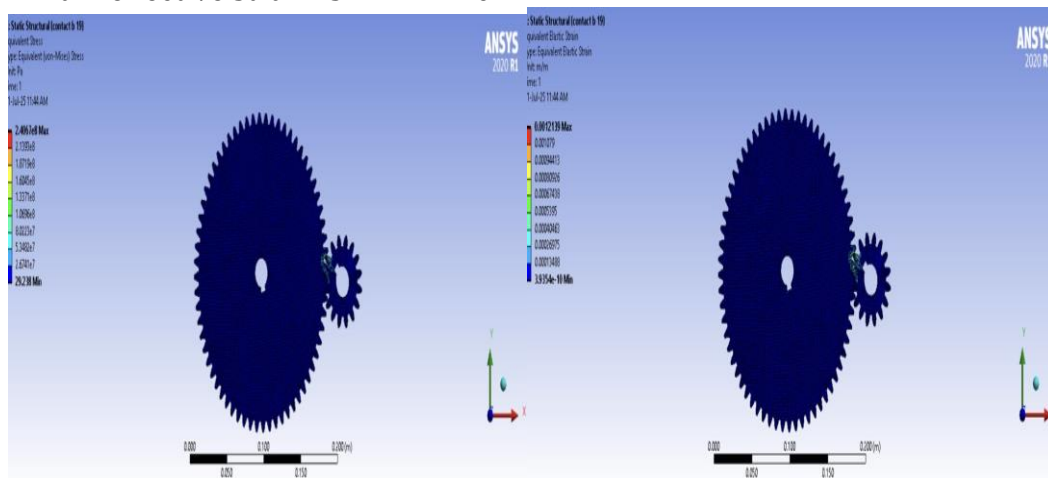


Figure 11. Equivalent Contact Stress and Strain (ASTM A 220-99)19 mm face width

In the numerical analysis of 21 mm face width spur gear set using (ASTM A 220-99) cast iron, the maximum von-Mises stress of spur gear set is 221.81 MPa and maximum effective strain is 1.126×10^{-3} .

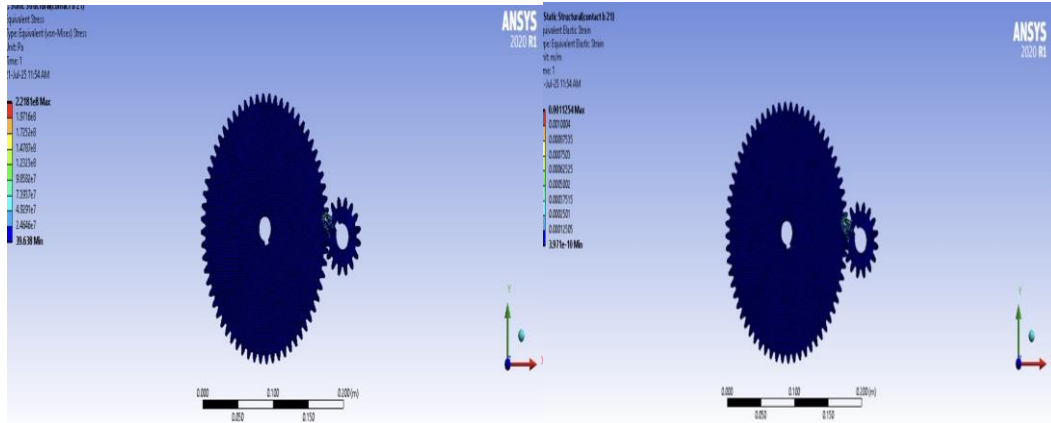


Figure 12. Equivalent Contact Stress and Strain (ASTM A 220-99)21 mm face width

In the comparison of results for face widths spur gears set, the results of von-Mises stress and effective strain of the (ASTM A 220-99) cast iron for the 21 mm face width spur gear set are less than those for (13,15,17,19) mm face widths. So, the 21 mm face width spur gear set is more suitable of gear than the other face widths. This can be seen in Table 5.

Table 5. Numerical Contact Stress and Effective Strain Result with Three Different Materials

Parameter	ASTM A 220-99	ASTM A 536-84	C54400
Von-Mises Stress [MPa]	247.42	256.65	265.87
Strain [$\times 10^{-5}$]	1.238	1.343	1.425

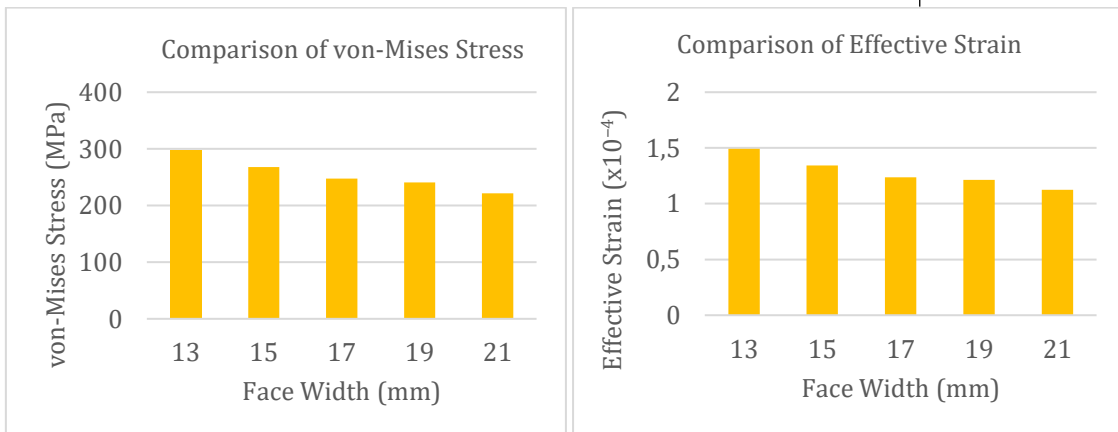


Figure 10. Comparison of Numerical Von-mises Stress and Effective Strain Result

D. Result and Discussion

In this study, spur gear sets with different materials and face widths are investigated. This study contains the contact stress and strain results of theoretical calculations and numerical work obtained from the AGMA equations and FEA, respectively. The minimum values of equivalent contact stress (247.42 MPa) and strain (1.238×10^{-3}) are taken from ASTM A 220-99. In order to achieve the required

objectives in this study, the five face widths of spur gear set geometry are changed by using ASTM A 220-99.

Table 6 and Figure 11 show the comparison of numerical results of von Mises stress and effective strain with different face widths (13 mm, 15 mm, 17 mm, 19 mm, and 21 mm). The maximum values are found in the 13 mm face width. The minimum values are found in the 21 mm face width. It has been noted that when face width increases, the maximum contact stress decreases.

Table 6. Numerical Contact Stress and Effective Strain Results by Changing Face Width

Face Width (mm)	Contact Stress (MPa)	Effective Strain (10^{-3})
13	297.65	1.492
15	268.14	1.343
17	247.42	1.238
19	240.67	1.214
21	221.81	1.126

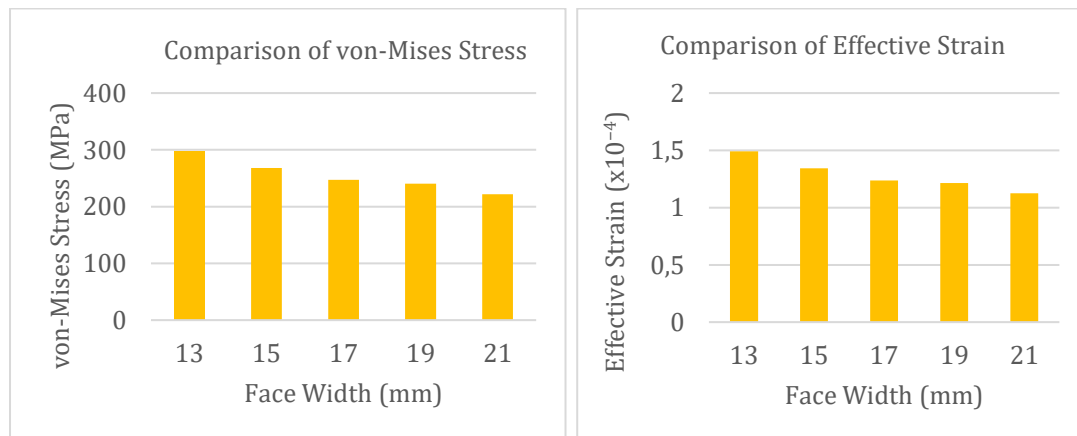


Figure 11. Comparison of Numerical Von-mises Stress and Effective Strain Result (Different Face Widths)

E. Conclusion

The module 2.5 mm and pitch diameter 48 mm spur gear set is used for this machine. The design of the gear set is expressed by changing three different materials (ASTM A 220-99, ASTM A 536-84, and Bronze C54400). The finite element method (FEM) is used to validate gear design calculations that are based on AGMA. The maximum percentage error between the theoretical and numerical results is about 5.3%. According to the results, the minimum von-Mises stress of spur gear is 247.42 MPa and the minimum effective strain is 1.238×10^{-3} , which are found in ASTM A 220-99. So, ASTM A 220-99 cast iron is chosen for the spur gear set. Consequently, it can be concluded that the spur gear's design is safe in working conditions. Moreover, it can be seen that the greater the face width, the smaller the von-Mises stress. And the smaller the face width, the greater the von-Mises stress and effective strain. So, the moderate value of face width (17 mm) is selected by considering power consumption and strength points of view. When designing gears, the choice of material and face widths are essential geometrical factors that affect the condition of stresses.

F. Acknowledgment

Firstly, the author wishes to express his deep gratitude to the Ministry of Transport and Communications for granting his permission to pursue this Degree of Program of Doctor of Philosophy. The author especially grateful to his parents, they supported his emotionally and financially. The author also really thankful to all teachers from Department of Mechanical Engineering, Mandalay Technological University for their suggestion, advice, support and encouragement throughout this research.

G. References

- [1] Pratik Patil, Prof. Dipali Bhojar, "Development and Analysis of Flywheel Operated Manual Sugar Cane Juice Making Machine " *International Journal of Advanced Research in Computer and Communication Engineering*, ISO 3297:2007 Certified Impact Factor 8.102 Vol. 12, Issue 4, April 2023.
- [2] Popoola, E.O., Taiwo, A., Akande, F.B., and Olaniran, J.A., "Performance Evaluation of a Modified Sugarcane Juice Extractor" *Nigerian Journal of Engineering Science Research (NIJESR)*. Vol. 5, Issue 2, pp. 51-60, June, 2022.
- [3] N. Oji¹, S. A. Okaiyeto, Y. A. Unguwanrimi, A. M. Sada, S. I. Ogijo and J. B. Jonga, "Performance Evaluation of a Small-Scale Sugarcane Juice Extracting Machine", *Current Journal of Applied Science and Technology*, April, 2021.
- [4] Rachel Ugye and Oladele Ayodeji Kolade, "Design Parameters for a Sugar Cane Extractor", *American Journal of Engineering Research (AJER)*, Volume-8, Issue-6, pp-118-123, May, 2019.
- [5] Rahul Ambare, Harshal Garud, Rahul Gunjal, Omkar Chavan, Vaibhav Hande., "Design and development of Sugarcane Juicer Machine", *Proceedings of Conference on Advances on Trends in Engineering Projects (NCTEP-2019)*.
- [6] Uti Joseph Nduka, Adogbeji Victor Omoefe, Akinola Adebisi Olayinka, "Design and Construction of Sugarcane Juice Extracting Machine For Rural Community", *International Journal of Engineering Applied Sciences and Technology*, Vol. 4, Issue 4, ISSN No. 2455-2143, Pages 306-311, August, 2019.
- [7] Robert L. Mott, Edward M. Vavrek, Jyhwen Wang, *Machine Elements in Mechanical Design*, Sixth Edition, 2018.
- [8] S. S. Anusha, P. S. Reddy, P. Bhaskar, and M. Manoj, "Contact Stress Analysis of Helical Gear by Using AGMA and ANSYS," *International Journal of Science Engineering and Advance Technology, IJSEAT*, vol. 2, p. 12, 2014, [Online]. Available: www.ijseat.com
- [9] P. B. Sonawane, P. G. Damle, B. E. Mechanical, and J. Ssb't's Coe Bambhori, "Static Structural Analysis of Gear Tooth," *International Journal of Engineering and Techniques*, vol. 2, [Online]. Available: <http://www.ijetjournal.org>
- [10] D. Singh, "Structural Analysis of Spur Gear Using FEM," *International Journal of Mechanical Engineering and Technology*, vol. 7, no. 6, pp. 1-08, [Online]. Available: <http://iaeme.com/Home/journal/IJMET01editor@iaeme.com> <http://iaeme.com/www.jifactor.com>
- [11] M. Phyo Thu and N. Lin Min, "Stress Analysis on Spur Gears Using ANSYS Workbench 16.0," *International Journal of Science and Engineering Applications*, vol. 7- issue 08, pp. 208-213, 2018, ISSN: -2319-7560 2018.

- [Online]. Available: www.ijsea.com208
- [12] R. S. Khurmi and J. K. Gupta, "A Textbook for the Students of Machine Design," 2005. (p701-748)
- [13] M. Keerthi, K. Sandya, and K. Srinivas, "Static & Dynamic Analysis of Spur Gear using Different Materials," *International Research Journal of Engineering and Technology*, 2016, [Online]. Available: www.irjet.net
- [14] R. Kiran Kumar, R. Karun Kumar, and Y. Durga Bhavani, "Design and Analysis of Spur Gear Using Ansys," *JETIR*, 2021. [Online]. Available: www.jetir.org55
- [15] S. Bhattacharya and M. Tech, "Spur Gear Theory and Design." [Online]. Available: www.ijariie.com
- [16] R. L. Mott, E. M. Vavrek, and J. Wang, "Machine Elements in Mechanical Design".
- [17] R. G. Richard G. Budynas, J. Keith. Nisbett, and J. Edward. Shigley, "Shigley's Mechanical Engineering Design". McGraw-Hill, New York, 2011.
- [18] A. AKPOLAT, "Analysis of Contact Stresses in Spur Gears by Finite Element Method," *European Journal of Science and Technology*, pp. 539–545, Dec. 2019, doi: 10.31590/ejosat.629155.
- [19] D. S. Balaji, S. Prabhakaran, and J. Harish Kumar, "Analysis of Surface Contact Stress for A Spur Gear of Material Steel 15ni2cr1mo28," vol. 12, no. 22, 2017, [Online]. Available: www.arpnjournals.com
- [20] P. Dewanji, "Design and Analysis of Spur Gear," *International Journal of Mechanical Engineering and Technology*, vol. 7, no. 5, pp. 209–220, [Online]. Available: <http://iaeme.com>www.jifactor.com<http://iaeme.com>
- [21] U. Ul, H. Khan, and R. D. Shelke, "Static Stress Analysis of Spur Gear Using Composite Materials in Ansys Workbench 2021r2", *International Research Journal of Modernization in Engineering Technology and Science*, vol.4, 2022 [Online]. Available: www.irjmets.com
- [22] M. Shinde, M. Nikam, and M. Mulla, "Static Analysis of Spur Gear Using Finite Element Analysis," *IOSR Journal of Mechanical and Civil Engineering*, SICETE. [Online]. Available: www.iosrjournals.org
- [23] J. Kh. Mohammed, Y. Kh. Khdir, and S. Y. Kasab, "Contact Stress Analysis of Spur Gear Under the Different Rotational Speed by Theoretical and Finite Element Method," *Academic Journal of Nawroz University*, vol. 7, no. 4, p. 213, Dec. 2018, doi: 10.25007/ajnu.v7n4a292.
- [24] M. Jebran Khan, A. Mangla, and S. H. Din, "Contact Stress Analysis of Stainless Steel Spur Gears using Finite Element Analysis and Comparison with Theoretical Results using Hertz Theory," *International Journal of Engineering Research and Applications*, ISSN: 2248-9622, vol. 5, issue 4, (Part -5) April 2015, pp. 10-18. [Online]. Available: www.ijera.com
- [25] A. Mahammad, I. H. Shanono, "Analytical Contact Analysis Finite Element Analysis," *Applied Research and Smart Technology*, ISSN: 2722-9645, vol. 2, no 2, 2021, pp. 41-46.